# Laser photoelectron spectrometry of $Co^-$ and $Ni^-$

Reed R. Corderman, P. C. Engelking,[a] and W. C. Lineberger[b]

*Department of Chemistry, University of Colorado and Joint Institute for Laboratory Astrophysics, University of Colorado and National Bureau of Standards, Boulder, Colorado 80309*
(Received 27 November 1978)

The photoelectron spectra of the negative ions $Co^-$ and $Ni^-$ have been obtained with a fixed frequency cw ArII laser (488 nm). The electron affinity of cobalt is found to be $0.662 \pm 0.010$ eV, while that of nickel is $1.157 \pm 0.010$ eV, in excellent agreement with a previously reported value E.A.(Ni) = $1.15 \pm 0.15$ eV determined by threshold photodetachment. Resolution of both negative ion and neutral fine structure intervals is obtained, and results in the determination of $Co^-$: $^3F_4 - {}^3F_3 = 910 \pm 50$ cm$^{-1}$, $^3F_3 - {}^3F_2 = 650 \pm 50$ cm$^{-1}$ and $Ni^-$: $^2D_{5/2} - {}^2D_{3/2} = 1470 \pm 100$ cm$^{-1}$. The intensities of individual fine structure components are calculated from an angular momentum analysis of the photodetachment process and are compared with the experimental results. The fine structure intensities do not follow the $(2J'' + 1)$ $(2J' + 1)$ statistical weighting of the negative ion $(J'')$ and neutral $(J')$ spin–orbit states, but are much better represented by geometrical factors. The detachment of $s$ electrons is preferred to the detachment of $d$ electrons at 488 nm.

## I. INTRODUCTION

While transition metals play an important role in vast areas of chemistry and physics, accurate measurements of atomic transition metal electron affinities using the techniques of tunable laser photodetachment or laser photoelectron spectrometry are relatively few in number.[1–4] This is, in large part, due to serious limitations of conventional (i.e., gas discharge) negative ion sources when employed to produce negative ions of metal-containing species.[2] Progress in the study of metal-containing species has recently been made by examining negative ions produced in discharges of volatile organotransition metal complexes, e.g., $Fe(CO)_5$, $Co(CO)_3NO$, and $(\eta^5\text{-}C_5H_5)NiNO$. This approach is severely limited, however, both by degradation of the ion source using these materials, and the limited number of commercially available high-volatility metal complexes, all of which suffer from varying degrees of toxicity. Subsequently, we have developed a sputtering technique[5] to produce and measure the electron affinities of a wide variety of negative ions of atomic metals, metal oxides, and metal clusters.

Previously measured accurate atomic transition metal electron affinities include E.A. (Cr) = $0.68 \pm 0.05$ eV,[2,6] E.A. (Ni) = $1.15 \pm 0.15$ eV,[2,7] E.A. (Fe) = $0.164 \pm 0.035$ eV,[1] E.A. (Cu) = $1.226 \pm 0.010$ eV,[3] E.A. (Ag) = $1.303 \pm 0.011$ eV,[3] E.A. (Au) = $2.3086 \pm 0.0007$ eV,[4] and E.A. (Pt) = $2.128 \pm 0.002$ eV.[4] In the present study, we have measured the electron affinities of atomic cobalt and nickel. $Co^-$ was obtained by discharging $Co(CO)_3NO$, while $Ni^-$ was produced by sputtering a nickel surface at $\approx 1 \times 10^{-6}$ torr.[5]

Figure 1 shows the energy levels of atomic cobalt,[8] nickel,[8] and their respective negative ions. Photodetachment of these anions with an Ar II laser operating at 488 nm (2.54 eV) is energetically capable of producing neutral atoms either in ground states (Co $a^4F_{J'}$; Ni $a^3F_{J'}$) or in one of several excited states (Co $b^4F_{J'}$, $a^2F_{J'}$, or $a^4P_{J'}$; Ni $a^3D_{J'}$ or $a^1D_2$). Thus, the photodetachment spectrum of cobalt should consist of four well-separated groups of peaks, while that for nickel should display two groups of peaks, with one group made up of the overlapping $a^3F_{J'}$ and $a^3D_{J'}$ states. The electron affinity is defined[9] as the minimum energy required to remove an electron from a negative ion in the lowest energy level of the ground electronic state, producing a neutral atom in the lowest energy level of its ground electronic state. The electron affinity of cobalt is thus the difference between the $Co^-$ $^3F_4$ and Co $a^4F_{9/2}$ levels, and for nickel that between the $Ni^-$ $^2D_{5/2}$ and Ni $a^3F_4$ levels. The photoelectron spectra presented here permit determination both of these electron affinities, and of the spin–orbit splittings in the negative ions. The measured intensities for individual fine structure transitions are compared with those calculated from an angular momentum analysis of the photodetachment process.[10–15]

## II. EXPERIMENTAL

The instrumentation and experimental techniques of laser photoelectron spectrometry have been previously discussed in detail.[16] Cobalt tricarbonyl nitrosyl (Strem Chemicals, Danvers, MA) is dissociated in a low pressure electrical discharge ion source[17] to produce a beam of $Co^-$ ions. A negative ion beam of $Ni^-$ is produced by a cesium beam sputter ion source (described below). The ions are extracted from the source, accelerated to 680 eV, focused, and the ion of interest is mass selected by a Wien filter.[18] The $\approx 0.3$ nA mass selected ion beam is crossed in a field-free interaction region by the linearly polarized intracavity beam of a cw argon-ion laser operating at 488 nm (2.540 eV). Electrons photodetached into a small solid angle ($6.28 \times 10^{-3}$ sterad) perpendicular to both the negative ion and photon beams enter a hemispherical electron monochromator and are energy analyzed (resolution 55 meV FWHM). The centers of individual peaks can be determined generally to $\pm 5$ meV.

The absolute, center-of-mass, electron kinetic energies of peaks in the photodetachment spectra are determined using simultaneously produced $O^-$ as a calibration ion and the expression[16]

---

[a] Present address: Department of Chemistry, University of Oregon, Eugene, OR 94703.

[b] Camille and Henry Dreyfus Teacher–Scholar.

 0021-9606/79/104474-07$01.00 

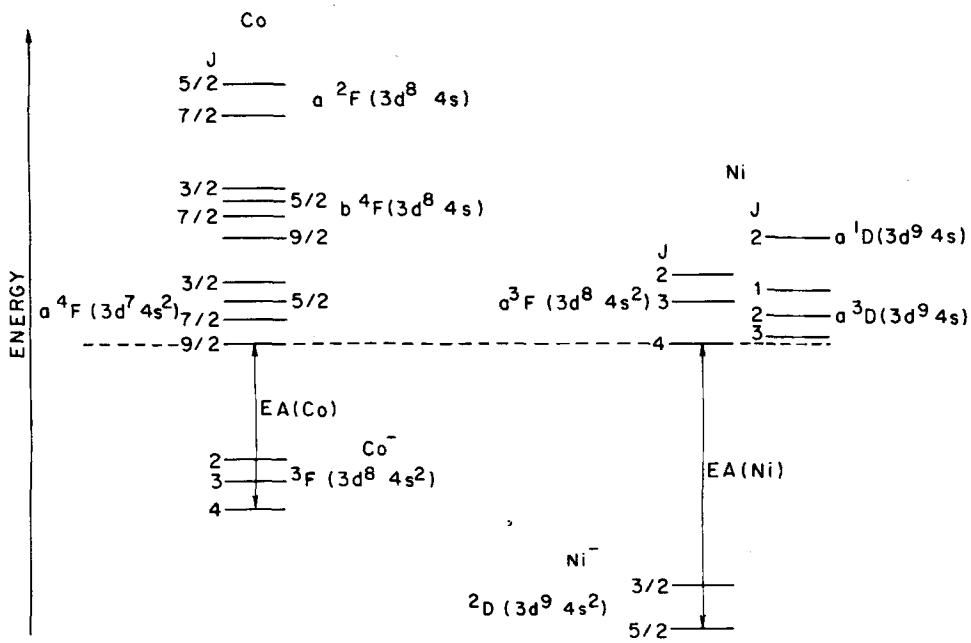


FIG. 1. Schematic of atomic energy levels in Co, Ni, $Co^-$, and $Ni^-$ observed in this experiment. Absorption of a 2.54 eV photon (488 nm) can detach an electron from $Co^-$ or $Ni^-$ and leave the resulting atom in any of the neutral states shown.

$$E_x = 2.540\ \text{eV} - \text{E.A.(O)} - \gamma(\Omega_{O^-} - \Omega_{X^-}) - mW(1/M_O - 1/M_X)\,, \quad (1)$$

where E.A.(O) = 1.465 eV is the "effective" electron affinity of the oxygen atom,[3,17] determined from the center of the $O^-$ photodetachment peak; $\gamma$ is an energy scale compression factor described previously,[16] determined by calibrating an $NH^-$ photodetachment spectrum against the known values for the NH $a^1\Delta - X^3\Sigma$ splitting[19]; and $(\Omega_{O^-} - \Omega_{X^-})$ is the laboratory energy difference between the $O^-$ peak center and a particular $X^-$ peak center. The final term in Eq. (1) is a consequence of the fact that an electron collected perpendicular to the ion beam must have been ejected in the center-of-mass frame backwards with respect to the ion beam direction,[16] $W$ is the kinetic energy of the ion beam (680 eV), and $m$, $M_O$, and $M_X$ are the masses of the electron, oxygen atom, and species X, respectively. All data were obtained with the laser polarization vector oriented at the "magic angle" (54°44') with respect to the electron collection direction.[20,21] The data thus represent an average photodetachment cross section, independent of the angular distribution of the detached electrons.[9,22,23]

The sputter ion source used in these experiments is a scaled down version of a Middleton-type sputter source developed for use with tandem van de Graaf accelerators. Briefly, cesium positive ions are produced by heating to ≈1100 °C a β-eucryptite cesium salt ($Cs_2O \cdot Al_2O_3 \cdot 2SiO_2$) which has been fused into a porous tungsten disc (Spectra-Mat, Inc., Watsonville, CA).[24] The cesium ion beam (typically 100 μA) produced by surface ionization is accelerated to 4 keV and focused with an einzel lens onto a metal target with a small (1 mm) aperture, which permits extraction of the negative ions produced. In the present study, a nickel target was fabricated from 0.75 in. nickel rod shaped in the form of a hollow cone with the $Cs^+$ ion beam entering from its base. $Ni^-$ ions produced by sputtering are extracted through a 1 mm aperture at the apex, accelerated to 680 eV, focused, and mass selected as previously described.[16]

## III. RESULTS AND DISCUSSION

### A. Cobalt

The $Co^-$ photodetachment spectrum measured at 2.54 eV photon energy (488 nm) is presented in Fig. 2. From a spectrum which may contain 22 transitions, involving the three fine structure levels of $Co^-$ $^3F_J$, and the three

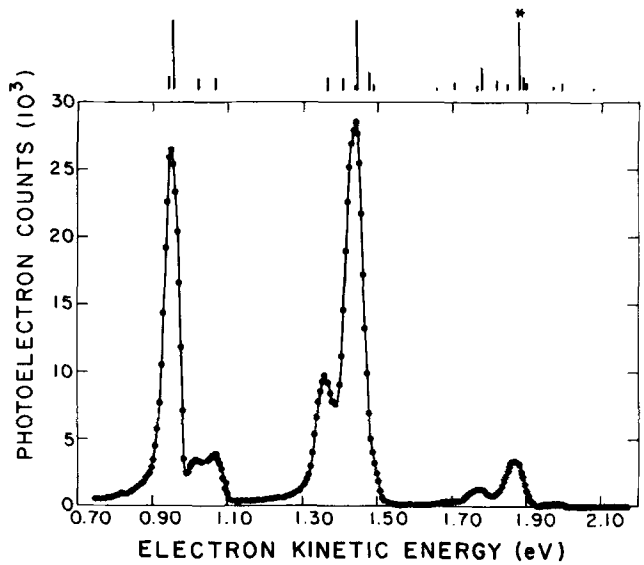


FIG. 2. The cobalt photodetachment spectrum taken at 488 nm (discharge source). The energy scale denotes the center-of-mass electron kinetic energy. The vertical lines above the spectrum indicate the location and calculated intensity ratio (Table I) for the allowed transitions. The location of the transition $Co^-$ $^3F_4 \rightarrow Co$ $a$ $^4F_{9/2}$ which gives the electron affinity is indicated by an *. The observed $d$-electron photodetachment intensities are approximately one tenth the intensities of the $s$-electron photodetachment peaks.

energetically accessible terms of neutral cobalt, we resolve nine distinct photodetachment peaks in three groups. The assignment of the various $J'' \rightarrow J'$ fine structure components is fairly straightforward, both by comparison of the observed spectrum with the well-known Co neutral spectrum,[8] and from the assumption that the peaks with the greatest intensity result from transitions between fine structure levels with the greatest relative population (i.e., lowest-lying levels). The intensity of each fine-structure transition is discussed in greater detail below. The Co $a^4P_{J'}$ state is not observed due to the cutoff of low-energy electrons by the electron monochromator (electron kinetic energy $< 0.25$ eV).

This identification now permits the determination of the electron affinity and negative-ion fine structure splittings. Both the $Co^-\ ^3F_4 \rightarrow$ Co $b^4F_{9/2}$ and $Co^-\ ^3F_4 \rightarrow$ Co $a^2F_{7/2}$ transitions at 1.446 and 0.955 eV electron kinetic energy, respectively, directly yield E.A.(Co) $= 0.662 \pm 0.010$ eV. Estimates of E.A.(Co) include $0.94 \pm 0.15$ eV from the calculation of Clementi,[25] 1.06 eV from the horizontal analysis of Zollweg,[26] 0.7 eV from Charkin and Dyatkina,[27] who employed the Glockler method,[28] 0.65 eV from Hotop *et al.*,[3] and $0.7 \pm 0.2$ eV from Hotop and Lineberger.[9]

The $Co^-$ fine structure splittings are directly determined by subtraction of the various $Co^-\ ^3F_{J''} \rightarrow$ Co $a^2F_{J'}$ components. The $^3F_{J''} \rightarrow a^4F_{J'}$ transition was not used to calculate $E(^3F_3 - {}^3F_4)$ because the peaks involved are pulled by partially overlapping transitions (Fig. 2). The difference in electron kinetic energy between the $Co^-\ ^3F_3 \rightarrow$ Co $a^2F_{7/2}$ and the $Co^-\ ^3F_4 \rightarrow$ Co $a^2F_{7/2}$ transitions gives $E(^3F_3 - {}^3F_4) = 910 \pm 50$ cm$^{-1}$; similarly, the ($Co^-\ ^3F_2 \rightarrow$ Co $a^2F_{5/2}$) − ($Co^-\ ^3F_3 \rightarrow$ Co $a^2F_{5/2}$) difference yields $E(^3F_2 - {}^3F_3) = 650 \pm 50$ cm$^{-1}$. These values are approximately $71\% \pm 3\%$ of the fine structure splittings observed in the atomic Ni $a^3F(3d^84s^2)$ term,[8] where $E$(Ni $a^3F_3 - a^3F_4$) $= 1332.153$ cm$^{-1}$ and $E$(Ni $a^3F_2 - a^3F_3$) $= 884.366$ cm$^{-1}$, and compare favorably with values of 980 and 650 cm$^{-1}$ obtained from extrapolation in the isoelectronic series $Co^-$, Ni, and $Cu^+$.

While the intensities of the $Co^-\ ^3F \rightarrow$ Co $b^4F$ and $Co^-\ ^3F \rightarrow$ Co $a^2F$ $s$-electron photodetachment transitions are comparable, the intensity of the $Co^-\ ^3F \rightarrow$ Co $a^4F$ transition, which involves the photodetachment of a $d$ electron, is reduced by an order of magnitude. An explanation of the reduced intensity for $d$-electron photodetachment relative to $s$-electron photodetachment has been previously proposed[1] for $Fe^-$. In this case, it is presumed that five of the seven $d$ electrons in $^4F(3d^74s^2)Fe^-$ remain coupled together, permitting only two $d$ electrons to detach from the negative ion, giving the correct $^5D(3d^64s^2)$Fe spin− and orbital−angular momentum ground state. Thus, while the $d$ electrons outnumber the $4s^2$ valence electrons, those able to leave the ion in a one-electron process are equal in number to the $s$-electrons and enjoy no statistical advantage. If one of these five $d$ electrons is photodetached, on the other hand, a plethora of triplet $(3d^64s^2)$Fe states results, the lowest of which[8] at 18 378.215 cm$^{-1}$ ($a\ ^3P_2$) is not observed due to the cutoff of low-energy electrons by the electron monochromator.

For $Co^-$ and $Ni^-$, a similar situation arises. In each case, the lowest configuration produced by detachment of one of the tightly coupled $d$ electrons lies in a region just beyond observation with the present 488 nm argon-ion laser line. Thus, there is little experimental evidence to support the claim that the five $d$ electrons of the same spin are tightly coupled. Secondly, were this argument valid, it would be expected that the ratio of the $d$-electron photodetachment to $s$-electron photodetachment intensities would increase with increasing $d$-electron population, i.e., in the order $Fe^- < Co^- < Ni^-$. While this behavior is not observed, future experiments using the Ar III 363.8 nm (3.407 eV) laser line to study the photodetachment spectra of $Fe^-$, $Co^-$, and $Ni^-$ may resolve these questions since, for $h\nu = 3.407$ eV, the Fe $a^3P_{J'}$, Co $a^4P_{J'}$, and Ni $b^1D_2$ states are energetically accessible.

One explanation of the observed intensity ratios between different terms may be that the reduced matrix element for $s$-electron photodetachment

$$I_s \propto |\langle \phi_s | \hat{\mu} | \chi_p \rangle|^2 \tag{2}$$

is much larger than those for $d$-electron photodetachment

$$I_d \propto |\langle \phi_d | \hat{\mu} | \chi_p \rangle|^2 + |\langle \phi_d | \hat{\mu} | \chi_f \rangle|^2 , \tag{3}$$

where $\phi_{l'}$ represents a bound atomic orbital of orbital angular momentum $l'$, $\hat{\mu}$ is a one-electron operator usually taken to be the electric dipole moment operator, and $\chi_l$ is the final continuum state of atom + photoelectron with angular momentum $l$.[10-12] A similar disparity in band intensities has been previously noted in the He I photoelectron spectra of *bis*-cyclopentadienyl metal compounds,[29-31] and also in the photodetachment spectrum of $FeO^-$.[32] In both cases, peaks resulting from removal of an electron from a metal $d$ orbital are relatively weak compared to peaks arising from ligand and ligand−metal bonding electrons (predominantly $s$ and $p$ electrons[33-36]). Interestingly, the partial photoionization cross sections for $d$-like orbitals in $HgCl_2$, while smaller at 584 Å, become much larger than those for the $p$-like valence bands at 304 Å.[37] This observation, combined with the present results, confirms that the reduced matrix elements [Eqs. (2) and (3)] are strongly energy dependent.

The observed intensity ratios for the transitions between various fine structure levels (Table I), as measured for $Co^-$ (and $Ni^-$, discussed below), deviate strongly from statistical expectations

$$I(J'' \rightarrow J') \propto (2J'' + 1)(2J' + 1) . \tag{4}$$

They are, however, very close to the intensity ratios determined by purely "geometrical" factors[13,14] or angular momentum coupling coefficients. These reflect the probability for producing different $jj$-coupled final states from $LS$-coupled intermediate states, to which the $LS$-coupled initial states have been transferred in an electric dipole transition by the absorption of a photon. Rau and Fano[13,14] first derived an expression for the intensity of a one-electron photodetachment from an $LS$-coupled negative ion, without inclusion of the fractional parentage coefficient for forming the ion term by adding

TABLE I. $Co^- \rightarrow Co$ photodetachment electron kinetic energies and intensities.

| Transition | Center-of-mass electron kinetic energy | Observed intensity ratio | Calculated intensity ratio [Eqs. (5)–(7)] | Statistical intensity ratio [Eqs. (4) and (6)] |
|---|---|---|---|---|
| $^3F_2 \rightarrow a^4F_{9/2}$ | 2.075 | $\leq 0.005 \pm 0.005$ | 0.003 | 0.16 |
| $^3F_3 \rightarrow a^4F_{9/2}$ | 1.990 | $0.07 \pm 0.01$ | 0.10 | 0.38 |
| $^3F_2 \rightarrow a^4F_{7/2}$ | 1.970 | | 0.05 | 0.13 |
| $^3F_2 \rightarrow a^4F_{5/2}$ | 1.897 | 1.00 | 0.09 | 0.09 |
| $^3F_3 \rightarrow a^4F_{7/2}$ | 1.889 | | 0.22 | 0.30 |
| $^3F_4 \rightarrow a^4F_{9/2}$[a] | 1.877 | | 1.00 | 1.00 |
| $^3F_2 \rightarrow a^4F_{3/2}$ | 1.847 | | 0.10 | 0.06 |
| $^3F_3 \rightarrow a^4F_{5/2}$ | 1.816 | | 0.16 | 0.23 |
| $^3F_4 \rightarrow a^4F_{7/2}$ | 1.776 | $0.39 \pm 0.02$ | 0.36 | 0.80 |
| $^3F_3 \rightarrow a^4F_{3/2}$ | 1.766 | | 0.07 | 0.15 |
| $^3F_4 \rightarrow {}^4F_{5/2}$ | 1.703 | $0.12 \pm 0.03$ | 0.10 | 0.60 |
| $^3F_4 \rightarrow a^4F_{3/2}$ | 1.653 | $\leq 0.01 \pm 0.01$ | 0.007 | 0.40 |
| $^3F_2 \rightarrow b^4F_{5/2}$ | 1.489 | $0.07 \pm 0.04$ | 0.08 | 0.09 |
| $^3F_3 \rightarrow b^4F_{7/2}$ | 1.477 | 1.00 | 0.29 | 0.30 |
| $^3F_4 \rightarrow b^4F_{9/2}$[a] | 1.446 | | 1.00 | 1.00 |
| $^3F_2 \rightarrow b^4F_{3/2}$ | 1.442 | | 0.04 | 0.06 |
| $^3F_3 \rightarrow b^4F_{5/2}$ | 1.409 | $0.10 \pm 0.04$ | 0.16 | 0.23 |
| $^3F_4 \rightarrow b^4F_{7/2}$ | 1.364 | $0.19 \pm 0.01$ | 0.20 | 0.80 |
| $^3F_3 \rightarrow a^2F_{7/2}$ | 1.068 | $0.16 \pm 0.02$ | 0.16 | 0.38 |
| $^3F_2 \rightarrow a^2F_{5/2}$ | 1.022 | $0.09 \pm 0.03$ | 0.16 | 0.12 |
| $^3F_4 \rightarrow a^2F_{7/2}$[a] | 0.955 | 1.00 | 1.00 | 1.00 |
| $^3F_3 \rightarrow a^2F_{5/2}$ | 0.941 | $0.15 \pm 0.03$ | 0.22 | 0.28 |

[a]The strongest transition in each group, taken to be of strength 1.00.

an electron to the neutral term, its "parent." This coefficient was included by Cox and Orchard[10–12] and the intensity expression was subsequently modified[1] to include the $2J''+1$ degeneracy of the negative ion fine structure levels. Additional differences between the Rau[13,14] and Cox[10–12] predictions are related to the treatment of the orbital angular momentum of the final state (neutral atom + continuum electron). Since in the present experiments the angular momentum of the photodetached electron is not observed, both approaches give identical results.[15] The resulting expression[1,15] for the relative intensity for a fine structure component of a specific transition between $LS$ states is

$$I(J', J'') \propto \sum_{j=l-1/2}^{j=l+1/2} (2J''+1)(2J'+1)(2j+1) \begin{Bmatrix} S'' & L'' & J'' \\ 1/2 & l & j \\ S' & L' & J' \end{Bmatrix}^2, \quad (5)$$

where the common factors independent of $J$ {the reduced matrix elements [Eqs. (2) and (3)] and the fractional parentage coefficient} have been suppressed. It is important to note that $l$ [Eq. (5)] represents the orbital angular momentum of the bound electron which is to be photodetached, and that within this formalism, the calculated fine structure intensity ratios are independent of the angular momentum of the ejected electron (e.g., $p \rightarrow ks$, $kd$, etc.).[15] Equation (5) assumes all $J''$ levels of the initial negative ion have been populated by their degeneracy, i.e., $kT \gg$ fine structure splitting. Otherwise, a weighting function peculiar to the method of production of the negative ions, such as a Boltzmann factor $[\exp(-E_{J''}/kT)]$, must be applied to these relative intensities. The calculated intensity ratios presented in Table I are corrected in this manner. For example, the expression

$$\frac{I_{obs}(^3F_3 \rightarrow a^2F_{7/2})}{I_{obs}(^3F_4 \rightarrow a^2F_{7/2})} = \exp\{-[E(^3F_3) - E(^3F_4)]/kT\} \cdot \frac{I_{calc}(^3F_3 \rightarrow a^2F_{7/2})}{I_{calc}(^3F_4 \rightarrow a^2F_{7/2})} \quad (6)$$

was used to calculate a representative temperature for the $Co^-$ ions produced in the gas discharge source (1800 °K). This temperature was then employed to obtain the appropriate $J''$ state initial populations for transitions involving production of the $a^4F$, $b^4F$, and $a^2F$ states.

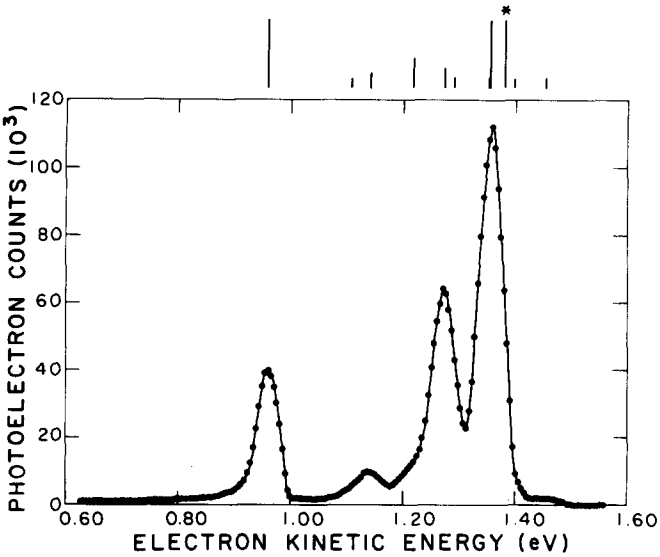


FIG. 3. The nickel photodetachment spectrum taken at 488 nm (sputter source). The energy scale denotes the center-of-mass electron kinetic energy. The vertical lines above the spectrum indicate the location and calculated intensity ratio (Table II) for the allowed transitions. The location of the $Ni^-\ ^2D_{5/2} \rightarrow Ni\ a\ ^3F_4$ transition which gives the electron affinity is indicated by an *. The observed $d$-electron photodetachment intensities are approximately one tenth the intensities of the $s$-electron photodetachment peaks.

One important selection rule is immediately found from the triangle relationship that the components of the $9-j$ coupling coefficient must satisfy[1,15,38,39] $|\Delta J| \leq l+\frac{1}{2}$.

For the special case of $l=0$, or the photodetachment of an $s$ electron, the $9-j$ symbol in Eq. (5) simplifies, and only one term remains in the intensity expression

$$I(J', J'') \propto (2J'+1)(2J''+1)\begin{Bmatrix} S'' & J'' & L'' \\ J' & S' & 1/2 \end{Bmatrix}^2, \qquad (7)$$

which may easily be evaluated by hand.[38,39]

## B. Nickel

The $Ni^-$ photodetachment spectrum measured at 2.54 eV photon energy (488 nm) is presented in Fig. 3. The spectrum was recorded using both the discharge source and the sputter source; no discernible differences were detected. From a spectrum which may contain 12 transitions between the two fine structure levels of $Ni^-\ ^2D_{J''}$ and the three energetically accessible terms of neutral Ni, we resolve five distinct photodetachment peaks in two groups, and observe three small shoulders on the larger features. As for cobalt, both comparison of the observed photodetachment spectrum with the well-known Ni neutral spectrum[8] and the assumption that the peaks with the greatest intensity result from transitions between lowest-lying states allow for immediate assignment of the various $J'' \rightarrow J'$ fine structure components (Table II). The $Ni^-\ ^2D_{J''} \rightarrow Ni\ a\ ^3F_{J'}$ $d$-electron photodetachment process occurs with much less intensity than either the $Ni^-\ ^2D_{J''} \rightarrow Ni\ a\ ^3D_{J'}$ or the $a\ ^1D_2$ $s$-electron photodetachments. Only small shoulders are observed for the $^2D_{5/2} \rightarrow a\ ^3F_4$, $^2D_{5/2} \rightarrow a\ ^3F_3$, and $^2D_{5/2} \rightarrow a\ ^3F_2$ transitions at $\approx 1.4$, $\approx 1.2$, and $\approx 1.1$ eV electron kinetic energy, respectively. As for iron[1] and cobalt, this behavior may be caused by significant differences between the reduced matrix elements for $s$- and $d$-electron photodetachment {Eqs. (2) and (3), respectively}.

The electron affinity of the $a\ ^3D_3$ level combined with the energy of this level above the $a\ ^3F_4$ ground state yields E.A.(Ni) = 1.157 ± 0.010 eV. As a check, subtracting the energy of the $a\ ^1D_2$ level from its electron

TABLE II. $Ni^- \rightarrow Ni$ photodetachment electron kinetic energies and intensities.

| Transition | Center-of-mass electron kinetic energy (eV) | Observed intensity ratio | Calculated intensity ratio [Eqs. (5)–(7)] | Statistical intensity ratio [Eqs. (4) and (6)] |
|---|---|---|---|---|
| $^2D_{3/2} \rightarrow a\ ^3F_4$ | 1.566 | ··· | 0.04 | 0.21 |
| $^2D_{3/2} \rightarrow a\ ^3F_3$ | 1.401 | ··· | 0.14 | 0.04 |
| $^2D_{5/2} \rightarrow a\ ^3F_4$[a] | 1.383 | 1.0 | 1.00 | 1.00 |
| $^2D_{3/2} \rightarrow a\ ^3F_2$ | 1.291 | ··· | 0.16 | 0.12 |
| $^2D_{5/2} \rightarrow a\ ^3F_3$ | 1.218 | 0.5 ± 0.2 | 0.43 | 0.78 |
| $^2D_{5/2} \rightarrow a\ ^3F_2$ | 1.109 | 0.3 ± 0.2 | 0.12 | 0.56 |
| $^2D_{3/2} \rightarrow a\ ^3D_2$ | 1.457 | 0.02 ± 0.01 | 0.14 | 0.14 |
| $^2D_{5/2} \rightarrow a\ ^3D_3$[a] | 1.358 | 1.00 | 1.00 | 1.00 |
| $^2D_{3/2} \rightarrow a\ ^3D_1$ | 1.353 | | 0.14 | 0.14 |
| $^2D_{5/2} \rightarrow a\ ^3D_2$ | 1.274 | 0.56 ± 0.01 | 0.29 | 0.29 |
| $^2D_{3/2} \rightarrow a\ ^1D_2$ | 1.143 | 0.22 ± 0.01 | 0.21 | 0.21 |
| $^2D_{5/2} \rightarrow a\ ^1D_2$[a] | 0.961 | 1.00 | 1.00 | 1.00 |

[a]The strongest transition in each group, taken to be of strength 1.00.

affinity also gives E.A.(Ni) = 1.157 ± 0.010 eV. This value agrees well with E.A.(Ni) = 1.15 ± 0.15 eV determined by Feldman *et al.*,[2,7] and is in reasonable agreement with other extrapolated or calculated values: 1.276 ± 0.020 eV (Clementi[25]), 1.1 eV (Charkin and Dyatkina[27]), 1.13 eV (Hotop *et al.*[3]), 1.62 eV (Zollweg[26]), and 1.15 ± 0.10 eV (Hotop and Lineberger[9]).

The $Ni^-$ fine structure splitting is determined from the difference of either the $^2D_{3/2} \rightarrow a^3D_2$ and $^2D_{5/2} \rightarrow a^3D_2$ transitions, or the $^2D_{3/2} \rightarrow a^1D_2$ and $^2D_{5/2} \rightarrow a^1D_2$ transitions. The average value is 0.182 ± 0.014 eV or 1470 ± 100 $cm^{-1}$. This agrees favorably with a $^2D_{5/2}-{}^2D_{3/2}$ splitting of 0.187 eV = 1509 $cm^{-1}$ determined by Zollweg.[26] As is the case for cobalt, this spin–orbit splitting is approximately 72% of that observed in the $4s^2\,{}^2D(3d^94s^2)$ term in atomic copper.[8]

While the observed intensity ratios for $Ni^-$ photodetachment deviate strongly from statistical expectations [Eq. (4)], the intensity ratios calculated from angular momentum considerations [Eqs. (5) and (7)] also deviate from the observed intensity ratios. These deviations occur in two distinct forms: First, the photodetachment peak representing the $^2D_{5/2} \rightarrow a^3D_2$ process seems anomalously large, with an observed intensity of 0.56 that of the $^2D_{5/2} \rightarrow a^3D_3$ transition, while the calculated intensity is 0.29; second, the $^2D_{5/2} \rightarrow a^1D_2$ transition appears small, as one would expect its absolute intensity to be approximately the same as the intensity of the $Ni^-\ {}^2D_{5/2} \rightarrow Ni\ a^3D_3$ transition. Note, for example, that the intensities of the $Co^-\ {}^3F_4 \rightarrow Co\ b^4F_{9/2}$ and $Co^-\ {}^3F_4 \rightarrow Co\ a^2F_{7/2}$ transitions are approximately equal (Fig. 2), as are the $Fe^-\ {}^4F_{9/2} \rightarrow Fe\ a^3F_{J'}$ and $Fe^-\ {}^4F_{9/2} \rightarrow Fe\ a^5F_{J'}$ transition intensities.[3] The first effect is most likely due to an interaction between the $a^3D_2$ and $a^1D_2$ state of neutral nickel, and is not completely unexpected in first-row transition metal elements with overlapping terms arising from $3d^X$, $3d^{X-1}s^1$, and $3d^{X-2}s^2$ configurations.[40] Indeed, calculations of the configuration mixing in neutral cobalt[41] show that while the $a^4F(3d^74s^2)$ and $b^4F(3d^84s)$ states may mix, the mixing coefficient is calculated to be only 0.0064, too small to perturb seriously the fine structure levels involved. On the other hand, the Ni $a^3D_2$ fine structure level at 879.8 $cm^{-1}$ is shifted by ≈ 300 $cm^{-1}$ from a position of 1109.8 $cm^{-1}$ calculated if the Ni $a^3D_{J'}$ multiplet ideally obeyed the Landé inverval rule.[40] The occurrence of configuration mixing between the $a^3D_2$ and $a^1D_2$ levels is further suggested by the observation of many emission bands in the arc spectrum of nickel from a common origin to both the $a^3D$ and $a^1D$ terms.[42]

In an attempt to quantify this argument, we assume that the interaction between the $a^3D_2$ and $a^1D_2$ states may be found by calculation of the normalized eigenvectors of the 2×2 secular determinant

$$\begin{vmatrix} E(^1D_2) - \lambda & AJ(J+1) \\ AJ(J+1) & E(^3D_2) - \lambda \end{vmatrix} = 0 , \tag{8}$$

where $E(a^1D_2) - \lambda = 3409.9\ cm^{-1}$, $E(a^3D_2) - \lambda = 879.8\ cm^{-1}$, $E(a^3D_2) = 1109.8\ cm^{-1}$, $AJ(J+1)$ represents the interaction term between the two levels, and $J = 2$. Solution of Eq. (8) gives the energy of the unperturbed $a^1D_2$ level $E(a^1D_2) = 3180.0\ cm^{-1}$, a mixing interaction energy $A = -121.2\ cm^{-1}$, and wave functions $\psi_p$ for the perturbed $a^1D_2$ and $a^3D_2$ states in terms of the unperturbed basis wave functions $\psi$:

$$\psi_p(a^1D_2) = 0.9535\psi(a^1D_2) - 0.3015\psi(a^3D_2) , \tag{9}$$

$$\psi_p(a^3D_2) = 0.3015\psi(a^1D_2) + 0.9535\psi(a^3D_2) . \tag{10}$$

These perturbed wave functions $\psi_p$, which represent approximately a 10% admixture of triplet character in the $a^1D_2$ level, may be used to recalculate the geometrical factors [Eqs. (5) and (7)] for the photodetachment process. The intensity of the $Ni^-\ {}^2D_{J'} \rightarrow Ni\ a^1D_2$ transition is given by

$$\begin{aligned} I(^2D_{J'} \rightarrow a^1D_2) &= |\langle k_p || \hat{\mu} || 0.9535\psi(a^1D_2) + 0.3015\psi(a^3D_2)\rangle|^2 = |\langle k_p || \hat{\mu} || \psi(a^1D_2)\rangle|^2(0.9535)^2 \\ &+ |\langle k_p || \hat{\mu} || \psi(a^3D_2)\rangle|^2(0.3015)^2 - 2\,\mathrm{Re}[\langle k_p || \hat{\mu} || \psi(a^1D_2)\rangle\langle k_p || \hat{\mu} || \psi(a^3D_2)\rangle](0.9535)(0.3015), \end{aligned} \tag{11}$$

where $\hat{\mu}$ is as before [Eqs. (2) and (3)] and $k_p$ is the angular momentum of the outgoing $p$ wave. If the $a^3D_{J'}$ and $a^1D_2$ states are assumed to have the same phase, then the matrix elements in Eq. (11) may be replaced by

$$\langle k_p || \hat{\mu} || \psi(a^1D_2)\rangle \cong 1 \tag{12}$$

and

$$\langle k_p || \hat{\mu} || \psi(a^3D_2) \cong 3\,\frac{\text{geom. factor}(a^3D_2)}{\sum \text{geom. factors}(a^3D_{J'})} , \tag{13}$$

where the geometrical factors are obtained from Eq. (7) for this $s$-electron photodetachment process (0.222 for the $a^3D_2$ level). Explicit evaluation of Eq. (11) for both $I(^2D_{5/2} \rightarrow a^1D_2)$ and $I(^2D_{5/2} \rightarrow a^3D_2)$ with these assumptions gives $I(^2D_{5/2} \rightarrow a^3D_2)/I(^2D_{5/2} \rightarrow a^3D_3) = 0.62$ compared to 0.56 observed experimentally (Table II), in much better agreement than the intensity ratio calculated from purely geometrical factors, or angular momentum considerations, alone. On the other hand, the intensity ratio of the $a^1D_2$ level compared to the $a^3D_2$ level is $I(^2D_{5/2} \rightarrow a^1D_2)/I(^2D_{5/2} \rightarrow a^3D_2) = 0.35$, while 0.63 is observed experimentally. This disagreement indicates that the absolute intensity of the $a^1D_2$ level is still small compared to that of the $a^3D_3$ level, and might be the result of a rapidly changing $s$-electron photodetachment cross section in the energy region from 0.9 to 1.3 eV, unlike the case for cobalt. Evidence for this change in cross section is provided by the measurements of Feldmann *et al.*,[2] who report a monotonically increasing photodetachment cross section for $Ni^-$ from threshold (≈ 1 eV) to ≈ 2 eV.

## IV. CONCLUSIONS

The electron affinities of Co(0.662 ± 0.010 eV) and Ni(1.157 ± 0.010 eV) have been directly measured by

laser photoelectron spectrometry of $Co^-$ and $Ni^-$, respectively. Partial resolution of both negative ion and neutral fine structure intervals is obtained, and results in the determination of $Co^-(^3F_4-{}^3F_3=910\pm 50\ cm^{-1}$, $^3F_3-{}^3F_2=650\pm 50\ cm^{-1})$ and $Ni^-(^2D_{5/2}-{}^2D_{3/2}=1470\pm 100\ cm^{-1})$. The intensities of individual fine structure components are calculated from an angular momentum analysis of the photodetachment process and are in good agreement with the experimental results.

## ACKNOWLEDGMENT

This work was supported in part by the National Science Foundation through grants CHE75-01565 and PHY76-04761 to the University of Colorado.

[1]P. C. Engelking and W. C. Lineberger, Phys. Rev. A 19, 149 (1979).
[2]D. Feldman, R. Rackwitz, E. Heinicke, and H. J. Kaiser, Z. Phys. A 282, 143 (1977).
[3]H. Hotop, R. A. Bennett, and W. C. Lineberger, J. Chem. Phys. 58, 2373 (1973).
[4]H. Hotop and W. C. Lineberger, J. Chem. Phys. 58, 2379 (1973).
[5]R. Middleton, Nucl. Instrum. Methods 144, 373 (1977); R. Middleton, IEEE Trans. Nucl. Sci. 23, 1098 (1976).
[6]D. Feldmann, R. Rackwitz, E. Heinicke, and H. J. Kaiser, Phys. Lett. A 45, 404 (1973).
[7]E. Heinicke, H. J. Kaiser, R. Rackwitz, and D. Feldmann, Phys. Lett. A 50, 265 (1974).
[8]C. E. Moore, "Atomic Energy Levels," NBS Circ. 467 (1948).
[9]H. Hotop and W. C. Lineberger, J. Phys. Chem. Ref. Data 4, 539 (1975).
[10]P. A. Cox and A. F. Orchard, Chem. Phys. Lett. 7, 273 (1970).
[11]P. A. Cox, S. Evans, and A. F. Orchard, Chem. Phys. Lett. 13, 386 (1972).
[12]P. A. Cox, in *Structure and Bonding* (Springer, Berlin, 1975), Vol. 24, pp. 59–81.
[13]A. R. P. Rau and U. Fano, Phys. Rev. A 4, 1751 (1971).
[14]A. R. P. Rau, in *Electron and Photon Interactions With Atoms*, edited by H. Kleinpoppen and M. R. C. McDowell (Plenum, New York, 1976), pp. 141–148.
[15]P. C. Engelking (to be published).
[16]M. W. Siegel, R. J. Celotta, J. L. Hall, J. Levine, and R. A. Bennett, Phys. Rev. A 6, 607 (1972); R. J. Celotta, R. A. Bennett, and J. L. Hall, J. Chem. Phys. 60, 1740 (1974).
[17]L. M. Branscomb, D. S. Burch, S. J. Smith, and S. Geltman, Phys. Rev. 111, 504 (1958).
[18]L. Wahlin, Nucl. Instrum. Methods 38, 133 (1965); 27, 55 (1964).
[19]P. C. Engelking and W. C. Lineberger, J. Chem. Phys. 65, 4323 (1976).
[20]J. L. Dehmer and J. Berkowitz, Phys. Rev. A 10, 484 (1974).
[21]P. Frey, F. Breyer, and H. Hotop, J. Phys. B 11, L589 (1978).
[22]J. Cooper and R. N. Zare, J. Chem. Phys. 48, 942 (1968).
[23]K. I. Reed, A. H. Zimmerman, H. C. Andersen, and J. I. Brauman, J. Chem. Phys. 64, 1368 (1976); E. P. Wigner, Phys. Rev. 73, 1002 (1948).
[24]O. Heinz and R. T. Reaves, Rev. Sci. Instrum. 39, 1229 (1968).
[25]E. Clementi, Phys. Rev. Sect. A 135, 980 (1964).
[26]R. J. Zollweg, J. Chem. Phys. 50, 4251 (1969).
[27]O. P. Charkin and M. E. Dyatkina, Zh. Struckt. Khim. 6, 422 (1965) [J. Struct. Chem. (USSR) 6, 397 (1965)].
[28]G. Glockler, Phys. Rev. 46, 111 (1934).
[29]S. Evans, M. L. H. Green, B. Jewitt, A. F. Orchard, and C. F. Pygall, J. Chem. Soc. Faraday Trans. 2 68, 1847 (1972).
[30]S. Evans, M. L. H. Green, B. Jewitt, C. King, and A. F. Orchard, J. Chem. Soc. Faraday Trans. 2 70, 356 (1974).
[31]K. D. Warren, in *Structure and Bonding* (Springer, Berlin, 1976), Vol. 27, pp. 45–159.
[32]P. C. Engelking and W. C. Lineberger, J. Chem. Phys. 66, 5054 (1977).
[33]A. K. Rappé and W. A. Goddard III, J. Am. Chem. Soc. 99, 3966 (1977).
[34]S. P. Walch and W. A. Goddard III, J. Am. Chem. Soc. 100, 1338 (1978).
[35]C. F. Melius, Chem. Phys. Lett. 39, 287 (1976).
[36]R. P. Messmer, D. R. Salahub, K. H. Johnson, and C. Y. Yang, Chem. Phys. Lett. 51, 84 (1977).
[37]J. Berkowitz, J. Chem. Phys. 61, 407 (1974).
[38]B. L. Silver, *Irreducible Tensor Methods—An Introduction for Chemists* (Academic, New York, 1976).
[39]D. M. Brink and G. R. Satchler, *Angular Momentum* (Oxford University, London, 1968), 2nd edition.
[40]E. U. Condon and G. H. Shortley, *The Theory of Atomic Spectra* (Cambridge University, London, 1964).
[41]E. -K. Viinikka and Y. Öhrn, Phys. Rev. B 11, 4168 (1975).
[42]H. N. Russell, Phys. Rev. 34, 821 (1929).